Received: 14 April 2020 | Revised: 15 January 2021 | Accepted: 15 March 2021

DOI: 10.1111/mec.15899

ORIGINAL ARTICLE

MOLECULAR ECOLOGY WILEY

Characterization of the microbiome and immune response in corals with chronic *Montipora* white syndrome

Tanya Brown[1] | Dylan Sonett[2] | Jesse R. Zaneveld[2] | Jacqueline L. Padilla-Gamiño[1]

[1]School of Aquatic and Fisheries Sciences, University of Washington, Seattle, Washington, USA

[2]Division of Biological Sciences, University of Washington, Bothell, Washington, USA

Correspondence
Tanya Brown, School of Aquatic and Fisheries Sciences, University of Washington, Seattle, WA 98105, USA.
Email: tanyabrown980@gmail.com

Funding information
Division of Integrative Organismal Systems, Grant/Award Number: 1655682

Abstract

Coral diseases have increased in frequency and intensity around the tropics worldwide. However, in many cases, little is known about their etiology. *Montipora* white syndrome (MWS) is a common disease affecting the coral *Montipora capitata*, a major reef builder in Hawai'i. Chronic *Montipora* white syndrome (cMWS) is a slow-moving form of the disease that affects *M. capitata* throughout the year. The effects of this chronic disease on coral immunology and microbiology are currently unknown. In this study, we use prophenoloxidase immune assays and 16S rRNA gene amplicon sequencing to characterize the microbiome and immunological response associated with cMWS. Our results show that immunological and microbiological responses are highly localized. Relative to diseased samples, apparently healthy portions of cMWS corals differed in immune activity and in the relative abundance of microbial taxa. Coral tissues with cMWS showed decreased tyrosinase-type catecholase and tyrosinase-type cresolase activity and increased laccase-type activity. Catecholase and cresolase activity were negatively correlated across all tissue types with microbiome richness. The localized effect of cMWS on coral microbiology and immunology is probably an important reason for the slow progression of the disease. This local confinement may facilitate interventions that focus on localized treatments on tissue types. This study provides an important baseline to understand the interplay between the microbiome and immune system and the mechanisms used by corals to manage chronic microbial perturbations associated with white syndrome.

KEYWORDS
16S rRNA, coral disease, innate immunity, microbiome, white syndrome

1 | INTRODUCTION

Coral reefs are among the most diverse and productive ecosystems in the world (Connell, 1978; Odum & Odum, 1955; Reaka-Kudla, 1997). However, coral reefs are declining rapidly due to global climate change and increased frequency and severity of disease outbreaks globally (Harvell & Lamb, 2020; Harvell et al., 2002; Lafferty et al., 2004; Peters, 2015; Plowright et al., 2008; Pollock et al., 2011; Sutherland et al., 2004). Despite the high incidence and prevalence of coral diseases and their devastating impacts on coral reefs, little is known about the mechanisms of pathogen transmission and defense, as well as agents responsible for infection (Bruno et al., 2007; Kline & Vollmer, 2011). *Montipora* white syndrome (MWS) is a disease that results in tissue loss in the reef building coral, *Montipora*

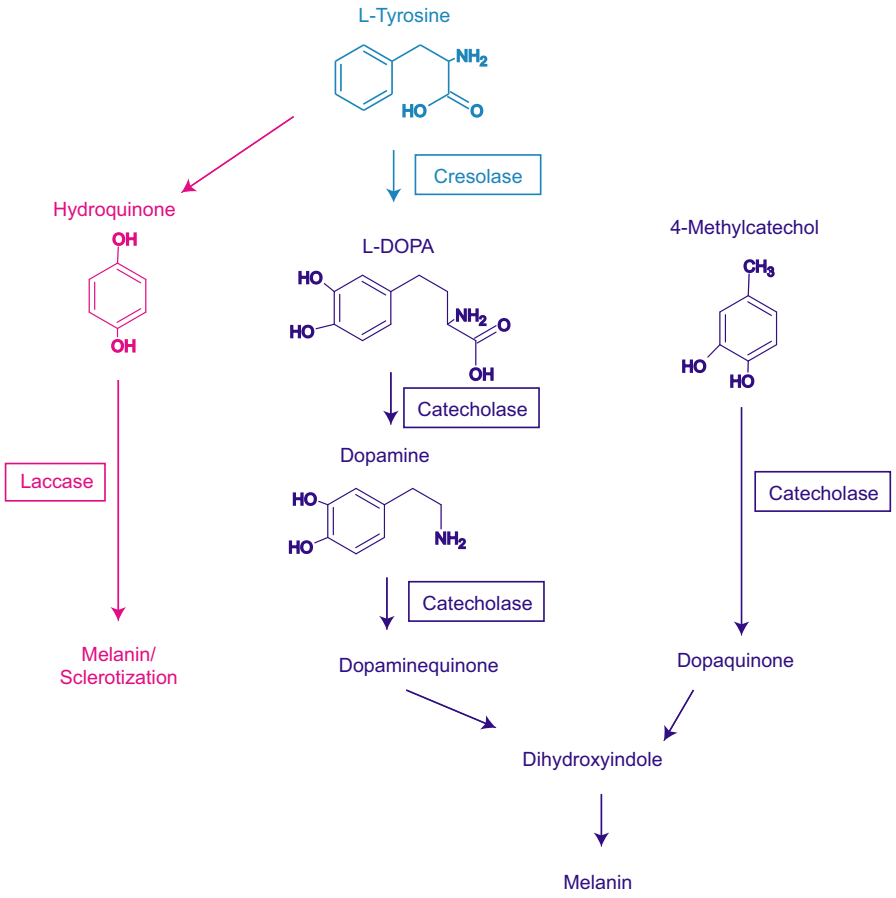

FIGURE 1 Depiction of the hypothesized melanin synthesis pathway in *M. capitata* with reference from insects. Components of the pathway measured in this study have their chemical structure illustrated. Cresolase activity was measured using L-tyrosine activity (blue). Tyrosinase-type catecholase activity was measured using: dopamine, L-DOPA, and 4-methylcatechol (purple). Laccase-type activity was also studied as a potential component of the innate immune response by investigating the activity of hydroquinone (pink). Enzymes (catecholase, cresolase, or laccase) involved in the reactions are shown in a box

capitata. This disease has been predominantly reported in Hawai'i (Aeby, 2006; Friedlander et al., 2008) where several MWS outbreaks have been documented over the last decade (Aeby et al., 2010, 2016).

MWS can occur as a chronic, slow moving disease with widespread tissue loss (cMWS) (Ushijima et al., 2012), or as a fast-progressive tissue loss disease called acute MWS (aMWS) (Aeby et al., 2016; Ushijima et al., 2014). Although previous culture-dependent experiments have implicated two *Vibrio* species as causative agents of MWS (Ushijima et al., 2012, 2014), there are still many gaps in our understanding of how coral bacterial communities shift during pathogen invasion and the disease associated immune responses.

The coral holobiont is a complex association between the coral host and various partners, which can include diverse bacteria, archaea, microbial eukaryotes (most prominently endosymbiotic dinoflagellates of the family Symbiodiniaceae, but also others including fungi, endolithic algae, and apicomplexans), and viruses (Bentis et al., 2000; Bourne et al., 2016; Rohwer et al., 2002; Schlichter et al., 1997; Upton & Peters, 1986). The coral-associated bacterial community contributes to the health of the coral by providing a heterotrophic source of nutrition (Bak et al.,1998; Sorokin, 1973), as well as cycling of nitrogen (Shashar et al., 1994; Siboni et al., 2008), carbon, sulphur (Kimes et al., 2010), and phosphorus (Ferrier-Pages et al., 2016). These interactions depend on the homeostasis between the coral host and associated microorganisms and rely on the capacity of the immune system to recognize and accept mutualists and identify pathogens. Despite the importance of the coral-associated bacterial community to coral performance and function, there is a lack of knowledge of how the microbial community interacts with the immune system of the host.

All animals use the innate immune system for self/nonself-recognition and protection from invading microorganisms and parasites (Irving et al., 2004). The melanin synthesis pathway has been associated with immunity in invertebrates (Nappi & Ottaviani, 2000), including corals (Palmer et al., 2010). This pathway is triggered by pathogens causing the deposition of melanin around foreign entities or wounds to protect the host (Mydlarz et al., 2008; Mydlarz, McGinty et al., 2009; Palmer et al., 2011). In invertebrates, the melanin pathway is activated by the proteolysis of proenzymes leading to the cleavage of prophenoloxidase (proPO) and the formation of phenoloxidase (PO). In insects, PO activity has been shown to combat infection by pathogens by promoting host defensive mechanisms such as phagocytosis (Cerenius et al., 2008). Additionally, in *Drosophila* sp., increased PO activity increases resistance to fungal infection (Tang et al., 2006). Decreased PO activity has also been associated with increased disease occurrence in corals (Mydlarz & Palmer, 2011; Pollock et al., 2019) and it is hypothesized that PO activity is associated with coral disease susceptibility. Specifically, in WS infections in corals, PO activity is shown to be higher at the onset of disease and is probably a mechanism used by corals to slow down or stop the progression of disease (Pollock et al., 2019). However, studies to

date have only researched one enzymatic substrate in association with disease.

Synthesis of melanin (melanization) is an important innate immune response that can occur by the tyrosinase-type and the laccase-type pathways (Mydlarz & Palmer, 2011) (Figure 1). The tyrosinase-type melanin synthesis pathway is associated with wound healing (Palmer, Traylor-Knowles, et al., 2011). This pathway has been well studied in invertebrates but the role of the laccase-type pathway requires further research (Palmer & Traylor-Knowles, 2012). Laccase-type pathways are probably involved in reinforcing damaged tissue, clot formation, and exoskeleton reinforcement (sclerotization) in invertebrates (Arakane et al., 2005; Mydlarz & Palmer, 2011; Palmer et al., 2012; Palmer, Traylor-Knowles, et al., 2011). Both, the tyrosinase and laccase-type pathways have been found in corals (Palmer & Traylor-Knowles, 2012) and differing affinity to pathway substrates suggests preferential use of a particular melanin synthesis substrate (Mydlarz & Palmer, 2011).

In this study, we examine shifts in the microbial community and immune response in healthy and diseased coral tissues to better understand the mechanisms associated with the dynamics and progression of white syndrome disease in *M. capitata*. We measured the total potential PO (tpPO) activity in diseased and healthy tissues of *Montipora capitata* by using the melanization pathway as a proxy for immunocompetence (van de Water, Leggat, et al., 2015). The enzymatic pathway components tested in this study have been previously found in corals and show different affinities for the different coral substrates (Mydlarz & Palmer, 2011). However, this is the first study to examine multiple components of the PO pathway in diseased and healthy corals and to investigate laccase-type activity in corals in relation to disease. To better understand the link between the immune response and the dynamics of the microbial consortia, we examined the microbial community in healthy and diseased tissues associated with cMWS using 16S rRNA gene amplicon sequencing. Measuring both parameters in the same tissue sample allowed us to assess how immune responses are associated with the microbial community during cMWS. We hypothesize that cMWS will cause a shift in the microbial community, that healthy tissues will have higher enzyme activity as they are actively fighting the oncoming infection and that levels of the components of the PO pathway will be suppressed in the diseased tissues due to a severely compromised immune system. Results from this study provide important insight into how cMWS affects *M. capitata* at the microbial community level and how the corals use the PO pathway to combat this disease.

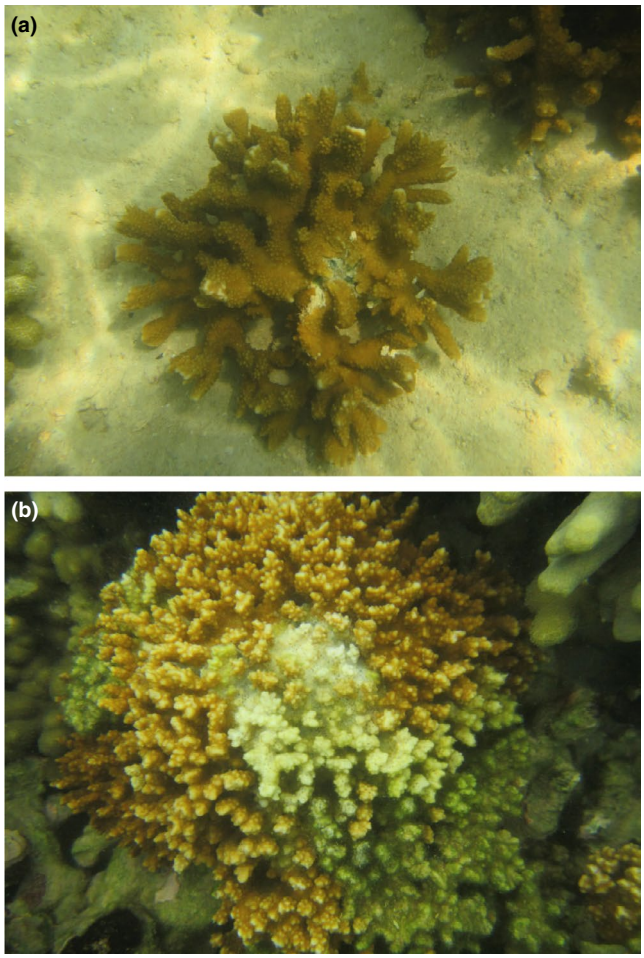

FIGURE 2 Two representative photographs of (a) a healthy *Montipora capitata* colony and (b) an infected *M. capitata* colony with cMWS. *M. capitata* exhibits high phenotypic plasticity (Forsman et al., 2010)

2 | MATERIALS AND METHODS

2.1 | Sample collection

Samples from *Montipora capitata* (2 cm in size) were collected from a patch reef located in Kāne'ohe Bay, O'ahu, Hawai'i on the east side of the Hawai'i Institute of Marine Biology (21.428°N, 157.792°W) in October, 2017. Samples were collected at a depth of approximately 1–2 m. Five healthy colonies (HT) and five colonies manifesting cMWS were sampled. For colonies manifesting cMWS, two samples were obtained, one from the diseased portion (WS) and another one from the healthy part of the tissue (WSH) (Figure 2). WS samples were collected 1 cm from the healthy/disease boundary while WSH samples were collected 2 to 3 cm from the healthy/disease boundary. Samples were snap frozen in liquid nitrogen immediately after collection and stored at −80°C until further analysis.

2.2 | Immune assays

Immunocompetence, the ability of an organism to elicit an immune response, was measured using five substrates in the PO pathway. The substrates used in this study were indicative of catecholase, cresolase, and laccase activities, which have been previously studied in several species of corals in the Caribbean (Mydlarz & Palmer, 2011). Tyrosinase-type catecholase activity was measured

using three substrates: dopamine, L-DOPA, and 4-methylcatechol. Tyrosine-type cresolase activity was measured using L-tyrosine. Laccase-type activity was also studied as a potential component of the innate immune response using hydroquinone as a substrate (Figure 1).

Coral immune assays were performed as previously described (Mydlarz et al., 2009; Mydlarz & Palmer, 2011; Palmer et al., 2011). Briefly, 2 ml of tissue slurry was obtained by airbrushing (IWATA Eclipse) the coral sample with extraction buffer (100 mM TRIS buffer +0.05 mM dithiothreitol). The slurry was homogenized on ice for 30 s using a hand-held tissue homogenizer (IKA Works) and centrifuged (15,000 *g*) for 10 min (Beckman Coulter) at 4°C to remove cellular debris. The supernatant was aliquoted and stored at −20°C for future analysis.

Protein concentrations were estimated using a Bradford assay (#23236, Thermo Fisher Scientific) with Coomassie G-250 dye (Bradford, 1976). Standards were created using bovine serum albumin (BSA; Pierce/Thermo Scientific) and protein concentrations were estimated by measuring the absorbance of the extracts at 595 nm and comparing them with the standard curve. Absorbances were quantified using a SPECTRAMAX M2 microplate reader (Molecular Devices).

PO immune assays were performed to target the previously identified components of the melanin synthesis pathway in triplicate by adding 20 µl of protein extract to a 96 well microtitre plate. Next, 50 µl of phosphate buffer (10 mM, pH 7.0) was added to the well followed by 20 µl of trypsin (0.2 mg/ml). Trypsin was added to the reaction to convert proPO into PO. This ensured the measurement of total potential PO (tpPO) activity. The plate was incubated for 30 min followed by the addition of 30 µl of L-tyrosine, dopamine, L-DOPA, 4-methylcatechol, or hydroquinone (10 mM stock) to the wells. The plate was read every five minutes for 30 min on a SPECTRAMAX M2 microplate reader (Molecular Devices) at 490 nm for assays with L-tyrosine, dopamine, L-DOPA, or hydroquinone as the substrate. Spectrophotometer readings were conducted at 410 nm for 4-methylcatechol. Enzymatic activities were calculated by subtracting the optical densities of the final reading from the initial reading and are presented as ΔOD per mg protein per min.

2.3 | DNA extraction

Total DNA was extracted using the Pure Link Plant Total DNA purification system (Invitrogen). Half centimeter coral samples (N = 15) were ground with a mortar and pestle in liquid nitrogen and then immediately transferred to 15 ml conical tubes containing 250 µl buffer R2. Then, samples were homogenized for 30 s using a tissue homogenizer (Tissue Ruptor, Qiagen) and immediately transferred to 1.5 ml centrifuge tubes. The Pure Link protocol was then followed. Sample purity was measured using a NanoDrop ND1000 spectrophotometer (NanoDrop Technologies). Samples showing good quality and concentrations were sent to Molecular Research LP for 16S rRNA amplicon sequencing.

2.4 | 16S rRNA gene amplicon sequencing

The V4 variable region of the 16S rRNA gene was amplified using the 515F (5′-GTGCCAGCMGCCGCGGTAA-3′) and 806R (5′-GGACTACHVGGGTWTCTAAT-3′) primer set (Caporaso et al., 2011). Amplification was conducted using a single-step 30 cycle PCR using HotStarTaq Plus Master Mix (Qiagen) under the following conditions: 94°C for 30 s, 53°C for 40 s, and 72°C for 1 min. A final elongation step at 72°C was conducted for 1 min. Sequencing was performed on an Ion Torrent PGM following manufacturers guidelines at Molecular Research LP. Sequences are deposited in NCBI as SRA project PRJNA662110. Initial sequencing resulted in collection of 1,162,455 total reads, with an average read depth of 77,497 (±34,928 SD) sequences per sample (Table S1A).

2.5 | Microbial sequence data quality control and initial processing

16S rRNA gene amplicon sequence data from Molecular Research LP were processed using the QIIME2 software package (Bolyen et al., 2019). All processing steps for quality control are available on GitHub (https://github.com/sonettd/MWS). The forward read from Molecular Research LP was imported into QIIME2 and demultiplexed (using the qiime cutadapt demux-single method). Sequences were then denoised and chimaera-checked (using the qiime dada2 denoise-pyro method) to generate amplicon sequence variants (ASVs) (Callahan et al., 2016). Because mitochondria and chloroplasts share common ancestry with free-living bacteria, but derive from host tissues, the presence of organelle SSU rRNA sequences can complicate microbial community analyses (D Sonett, T Brown, J Bengtsson-Palme, JL Padilla-Gamino, J Zaneveld in preparation). Therefore, we took care to identify such sequences during taxonomy annotation so they could be removed in silico prior to downstream analysis. To accomplish this, taxonomic annotations were assigned by q2 feature-classifier classify-consensus-vsearch using a custom reference taxonomy consisting of 99% OTUs from the SILVA 132 (Quast et al., 2012; Yilmaz et al., 2014) reference supplemented with coral mitochondria sequences from the Metaxa2 database (Bengtsson-Palme et al., 2015; DeSantis et al., 2006; Rognes et al., 2016). The percentage of sequences that derived from organelles ranged from <0.02% to ~77% between samples, emphasizing the importance of careful annotation of organelle sequences prior to analysis. Once annotated, chloroplast and mitochondria sequences were removed.

2.6 | Microbial community alpha and beta diversity analysis

Following quality control, we assessed microbiome alpha- and beta-diversity. In order to allow us to use phylogenetic alpha and beta diversity metrics, a fragment insertion approach was used to

insert short microbial 16S rRNA reads into a reference phylogeny. Sequences were placed on the QIIME2-compatible SILVA 128 tree included with the SEPP software using the qiime fragment-insertion sepp method (Quast et al., 2012; Yilmaz et al., 2014).

Alpha- and beta-diversity metrics were generated using the qiime diversity core-metrics phylogenetic method after rarefaction to 25,082 sequences per sample (the sequencing depth of the shallowest sample). Rarefaction reduces statistical power, but protects against false-positive results attributable to unequal sequencing depth between samples without the need to make strong assumptions about the distribution of microbial species within samples (Weiss et al., 2017). Alpha diversity was assessed using the number of unique observed ASVs in rarefied samples (a measure of community richness), Simpson's Evenness index (a measure of community evenness), and Shannon's diversity index (which combines richness and evenness). Overall differences in alpha diversity across health states were tested using Kruskal-Wallis tests. Post hoc comparisons were performed automatically in QIIME2 (via a procedure that produces equivalent *p*-values to a Mann-Whitney *U* post hoc test). The false discovery rate (FDR) for pairwise tests between health states was controlled using FDR q-values as reported by QIIME2. We assessed beta diversity between samples using Weighted UniFrac distances and Bray-Curtis dissimilarities. The significance of differences in beta-diversity between health states was tested using PERMANOVA (Anderson, 2001). Significant results in PERMANOVA may indicate either a change in mean community composition by health state (i.e., clustering) or alterations in dispersal (i.e., spread or variance). Therefore, PERMDISP was used to assess whether beta-diversity differences were driven by changes in dispersal.

2.7 | Joint analysis of microbial and immunological data

We sought to compare the overall pattern of changes in coral's immune parameters versus their associated microbial communities. To facilitate this, we manually constructed a table of the results of all immune assays (L-tyrosine, L-DOPA, dopamine, 4-methylcatechol, and hydroquinone used as substrates) in each coral sample. After Z-score normalizing the table so each assay contributed equally we then generated a Euclidean distance matrix from that table. In this distance matrix, coral samples with more divergent measurements in the immunological assays were assigned proportionally greater distances. This Euclidean distance matrix was then subjected to principal coordinates analysis for visualization. We also constructed individual distance matrices for each immune parameter to allow for separate testing.

To test for potential correlations between microbiome alpha diversity and innate immune parameters, microbiome richness (measured by observed ASV's in rarefied samples) and evenness (measured by Simpson's evenness index) were compared against health state and innate immune parameters using nonparametric tests. The Kruskal-Wallis test was used to test for associations between health state (WS, WSH, and HT) and alpha diversity while Spearman correlations were used to test for correlations between innate immune parameters and microbiome alpha diversity.

A weighted gene correlation network analysis (WGCNA) was conducted on bacterial count data and immune assay results to elucidate if any co-occurring clusters of bacterial families were mirroring innate immune parameters. The WGCNA R package (WGCNA V 1.69; Langfelder & Horvath, 2008)—most commonly used to analyse transcriptomic data—was employed here to infer co-occurring groups of bacteria ("modules") using a hierarchical clustering analysis on a correlation network created from the count-based microbial data. Default settings were used in running the package with minimal modification. When clustering microbial families, the minModuleSize was set to 10 and the mergeCutHeight was 0.9 with a soft threshold of 12. Module-trait relationships were then calculated from this initial clustering. In this analysis, a step-by-step network was constructed and modules were detected using the topology overlap matrix (TOM). In the end, similar modules were merged (minModuleSize =30) (Langfelder & Horvath, 2008). Final module–trait correlations output by WGCNA controlled for the FDR using the method of Benjamini–Hochberg.

2.8 | Statistical analysis of microbial taxonomy

All other statistical analyses of microbial taxonomy were conducted using SPSS V 26 (IBM). The top 10 bacterial families in each sample type (45 total families) were selected for taxonomic analysis. The significance of differences in relative abundance for bacterial families across the three health states were analysed with a generalized linear mixed model (GLMM) using colony as a random factor and tissue type as a fixed factor to determine differences at an $\alpha = 0.05$. The Benjamini-Hochberg FDR was used to control false discovery rate across bacterial families, and families with FDR $q < .05$ were taken as significant. Tests were used to compare healthy versus diseased tissue taking into account that WS and WSH samples came from the same coral colony. All three disease states were compared for all 45 families. Estimated marginal means were used to further compare differences in the relative abundance of bacterial families between health states. Additionally, swarm plots were generated to show the abundance of the top 10 bacterial families across health states using the SEABORN 0.11.0 python library (Waskom et al., 2020).

To assess whether any bacterial families or genera were indicators of particular health states (HT, WSH, WS) we used the INDICSPECIES package (version 1.7.9; De Caceres et al., 2016) in R.

2.9 | Statistical analysis of immunological parameters

Statistical analyses of immunological parameters were conducted using SPSS V 26 (IBM). PO activity assays (tyrosine, L-DOPA, dopamine, 4-methylcatechol, or hydroquinone) were averaged for the triplicate

runs. Immunity data were tested for normality and homoscedasticity using the Shapiro-Wilk's and Levene's tests respectively prior to performing statistical analyses. Differences in immune assays were assessed by health states with a general linear mixed model using individual as a random factor and tissue type (WS, WSH, and HT) as a fixed factor to determine differences at an $\alpha = 0.05$. Tests were used to compare healthy versus diseased tissue taking into account that WS and WSH samples came from the same coral colony. All three disease states were compared for the five immune assays. Estimated marginal means were used to further compare differences between health states within each of the five immune assays.

3 | RESULTS

3.1 | Immunocompetence

Proxies for immunocompetence–measured by enzymatic activity on L-DOPA, dopamine, 4-methylcatechol, L-tyrosine, and hydroquinone—revealed differences between health states in overall tyrosinase-type catecholase activity, tyrosinase-type cresolase activity, and laccase-type activity (Figure S1).

Tyrosinase–type catecholase activity was assessed by adding the activity of three enzymatic assays: L-DOPA, dopamine, and 4-methylcatechol as per Mydlarz and Palmer (2011). Similar to Palmer and et al. (2011), we found that different substrates testing for catecholase activity showed differing patterns across tissue types. In our study, overall catecholase activity was higher in WSH than HT samples (GLMM, $p = .016$, data not shown). Catecholase activity, using L-DOPA and dopamine as substrates, exhibited differences between health states (GLMM, $p = .002$, GLMM, $p = .005$, respectively, Figure 3a,b). Catecholase activity with L-DOPA as substrate showed lower activity in WS tissues than WSH (EMM, $p = .002$) and HT tissues (EMM, $p = .003$). Catecholase activity with dopamine as substrate showed higher activity in WSH tissue when compared to WS tissue (EMM, $p = .004$) and HT tissue (EMM, $p = .004$). There was no difference in activity in catecholase activity between tissues when 4-methylcatechol was used as a substrate (GLMM $p = .546$, Figure 3c).

Tyrosinase-type cresolase activity was measured using L-tyrosine as a substrate. Significant differences were observed between health

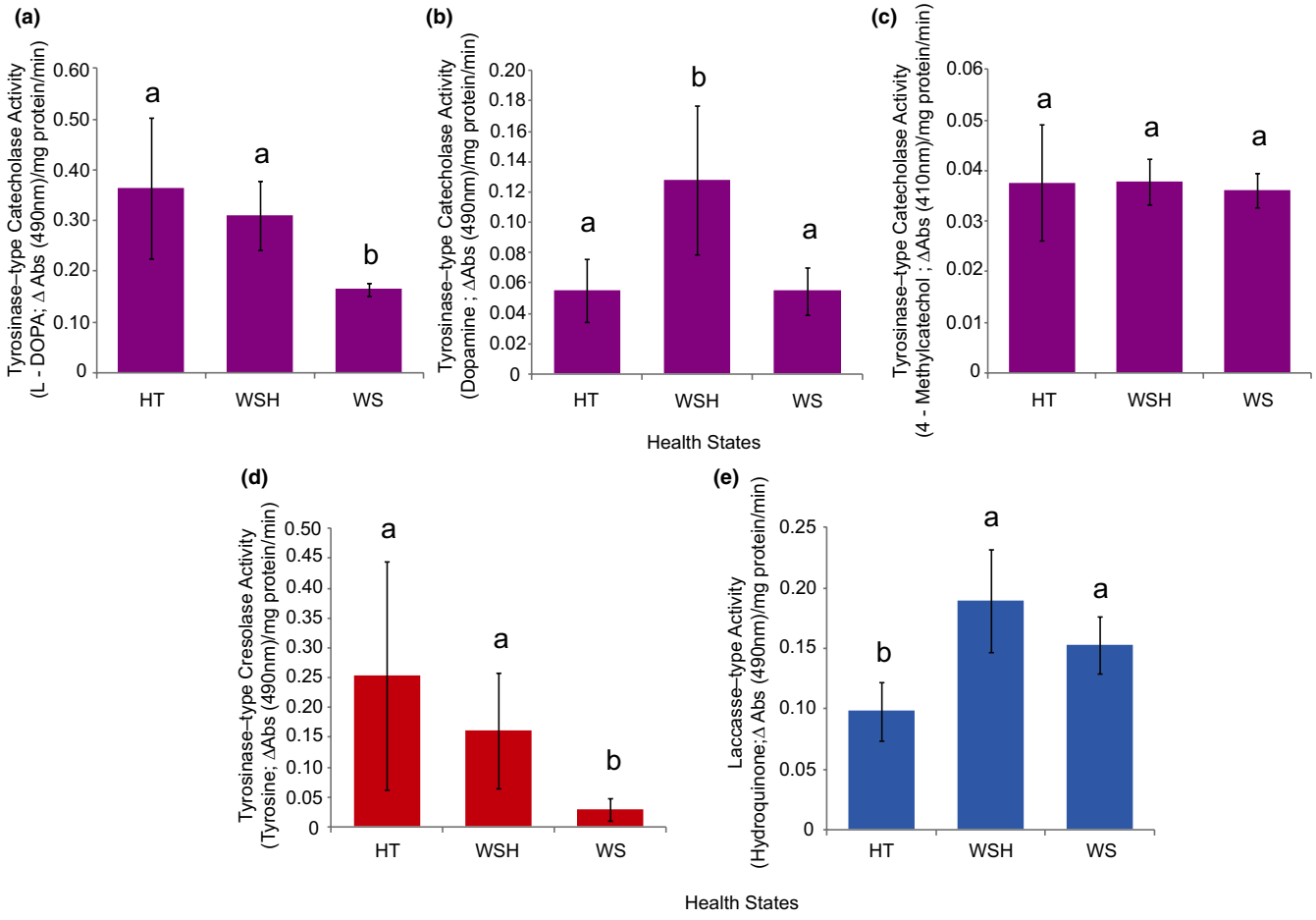

FIGURE 3 Substrate absorbance levels of L-DOPA (a), Dopamine (b), 4-Methylcatechol (c), Tyrosine (d), and Hydroquinone (e). Bar graph colours indicate enzyme type: tyrosinase-type catecholase-purple, tyrosinase-type cresolase-red, laccase-type-blue. Different letters over bars indicate significance ($p < .05$). Bars indicate standard error of the mean. HT, healthy colony; WS, diseased tissue in diseased colony; WSH, healthy tissue in diseased colony

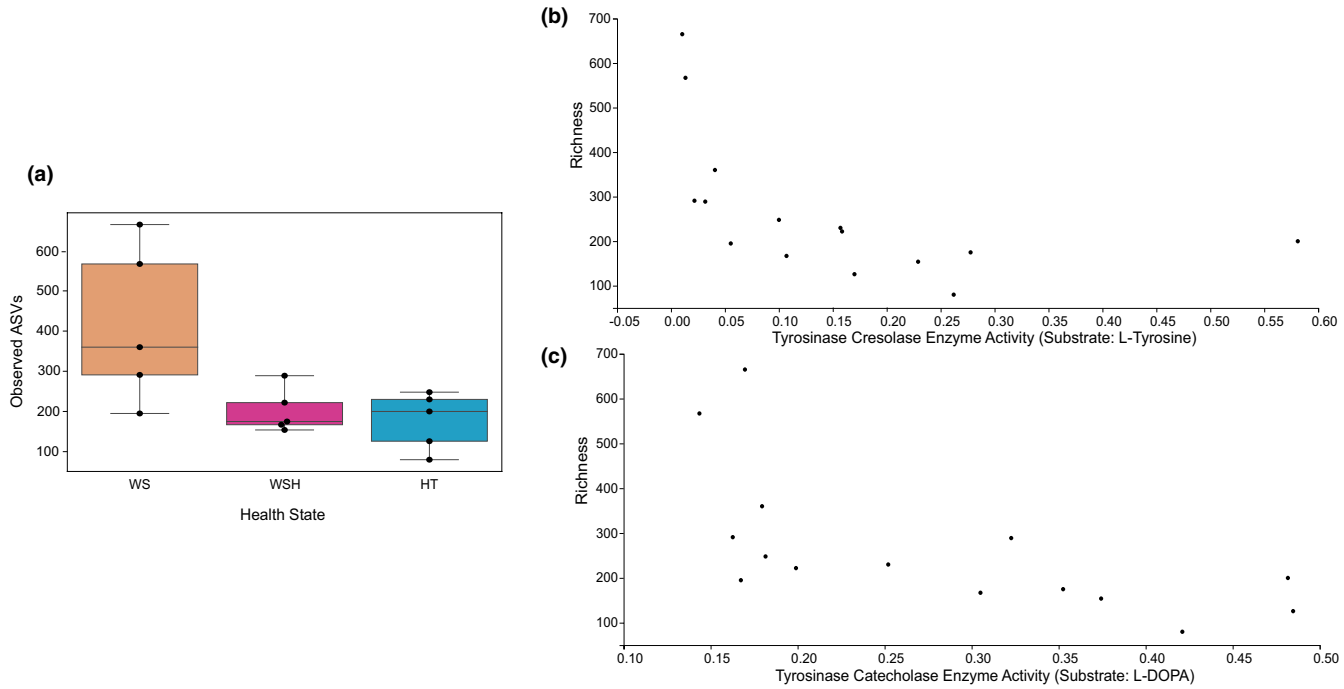

FIGURE 4 Relationship of microbiome richness relative to coral disease state and immunology. (a) Comparison of overall microbiome richness (observed ASVs in rarefied samples) with disease state. WS, diseased tissue in diseased colony (n = 5), WSH, healthy tissue in diseased colony (n = 5) and HT, healthy colony (n = 5). Diseased sections of diseased *Montipora capitata* colonies have nearly twice the microbiome richness as healthy individuals. (b) Comparison of microbiome richness with enzyme activity (L-tyrosine used as a substrate) levels. Corals with higher levels of enzyme activity showed lower levels of microbiome richness (Spearman r = −.8178, r^2 = .661, Bonferroni-corrected p = .00106), (c) Comparisons of microbiome richness with enzyme activity (L-DOPA used as substrate) levels. Corals with higher levels of enzyme activity showed lower levels of microbiome richness. (Spearman r = −.765, r^2 = .5856, Bonferroni-corrected p = .00513)

states (GLMM, p = .036, Figure 3d). Specifically, WS tissue showed lower activity than both healthy tissue types (WS vs. WSH, EMM, p = .038; WS vs. HT, EMM, p = .020) but no significant difference was found between WSH and HT tissue (EMM, p = .203).

Laccase-type activity was measured using hydroquinone as a substrate and differences in activity were found between heath states (GLMM, p < .0001 Figure 3e). Specifically, laccase-type activity was higher in WS (EMM, p = .017) and WSH tissues (EMM, p = .001) when compared to HT tissue. There was no difference in laccase-type activity when comparing tissue types on diseased colonies (WS vs. WSH, EMM, p = .089).

3.2 | Sequence quality control and removal of organelle sequences

We used high-throughput sequencing of 16S rRNA gene amplicons to compare microbial communities across disease states. After sequence quality control, including denoising, chimaera-checking and removal of chloroplasts and coral mitochondria, 538,105 total nonorganelle SSU rRNA gene sequences remained (Table S1A,B). The sequence with the fewest remaining reads had a read depth of 25,082 sequences (Table S1A). All samples were rarefied to that depth prior to statistical analysis.

3.3 | cMWS infected corals show increased microbiome richness but not evenness

We examined microbiome richness and evenness in three health states. Amplicon sequence variant (ASV) counts showed differences in microbial richness between health states (Kruskal-Wallis, p = .046; Table S2A,B). White syndrome (WS) tissues had on average roughly twice the richness of healthy tissue (HT), and ~1.8-fold the richness of apparently healthy portions of the same corals (WSH). However, pairwise comparisons were not significant (Kruskal-Wallis test FDR q = .07; Table S2).

We calculated Simpson's evenness index for each sample, and used this measure to analyse differences in evenness between samples (Table S2D). There were no significant differences in evenness across health states (Kruskal-Wallis, p = .54; Table S2E).

3.4 | Elevated L-tyrosine and L-DOPA correlate with low microbiome diversity

We compared the levels of each measured immune parameter with microbiome richness (Table S2C) and evenness (Table S2F). Higher levels of cresolase activity (measured using L-tyrosine) and higher levels of catecholase activity (measured using L-DOPA) were

strongly associated with lower levels of microbiome richness using Spearman correlation (L-tyrosine: Bonferroni-corrected p = .001, r = −.81, r^2 = .66; L-DOPA: Bonferroni-corrected p = .005, r = −.76, r^2 = .58; Figure 4; Table S2C). Indeed, results from either L-tyrosine or L-DOPA assays alone were sufficient to explain more than half of the variance in microbiome richness seen in this study (i.e., both r^2 > .5). Enzymatic activities measured using dopamine, 4-methylcatechol, and hydroquinone were not significantly correlated with microbiome richness (Table S2C). Microbiome evenness was not significantly correlated with any measured enzymatic activities (Bonferroni-corrected Spearman p = 1.0 for all samples; Table S2F).

3.5 | Beta-diversity ordination analysis

Ordination analysis of the ASV data revealed large differences in overall microbiome composition of corals with cMWS relative to healthy corals. Overall microbial beta-diversity differences between health status categories were significant using either Bray-Curtis dissimilarity or Weighted UniFrac (PERMANOVA; Table S3A). Based on visual inspection of PCoA plots, we thought there might be differences in dispersion across health states, which could reflect Anna Karenina Principle effects (Zaneveld et al., 2017). Although the elevated dispersion in cMWS tissue relating to healthy colonies was nominally significant before FDR correction for Bray-Curtis divergences (PERMDISP p = .019; Table S3B), we had compared all health states and therefore this nominal significance may be attributable to multiple comparisons (FDR q = .057). Moreover, no other significant differences in dispersion emerged in any combination of health states and beta-diversity metrics.

Both beta-diversity metrics showed most disease samples (WS) clustering away from samples from healthy coral colonies (HT) and the apparently healthy portions of diseased colonies (WSH). However, the details of this clustering differed somewhat based on the dissimilarity metric used. Using Bray-Curtis dissimilarity (a quantitative but nonphylogenetic measure of beta-diversity), three of the five WS tissue samples displayed a notably different bacterial community composition than the other bacterial community samples associated with *M. capitata* (Figure 5 and Figures S2, S3). Interestingly, these three samples (MWS1, MWS2, and MWS3) showed the greatest progression of disease. Using Weighted UniFrac (a quantitative phylogenetic measure of beta-diversity), microbiomes were found to be distinct between apparently healthy (HT or WSH) and diseased (WS) samples. Two outlying samples in the Weighted UniFrac beta-diversity analysis, WS5 and WSH5 showed unique microbial community composition relative to all other samples and each other. Samples that are outliers from a central cluster under Weighted UniFrac but not Bray-Curtis may reflect cases where a phylogenetically divergent microbe has increased or decreased in relative abundance. For example, sample WS5—an outlier in Weighted UniFrac—included 0.3% of class Acidomicrobia, >4-fold more than any other sample (Figures S4–S7, Table S4B). The converse case—in which a sample is an outlier in Bray-Curtis analysis but not Weighted UniFrac—may reflect a large change in relative abundance of one or more groups of microbes from well-represented taxa. Together these results show that cMWS alters the abundance and/or phylogenetic membership of coral microbiomes.

3.6 | Taxonomic analysis

In order to compare taxonomic changes by health state we first visualized taxonomic annotations of all taxa with >10 reads at multiple taxonomic levels (Figures S4–S11; Figure 6). Raw data on

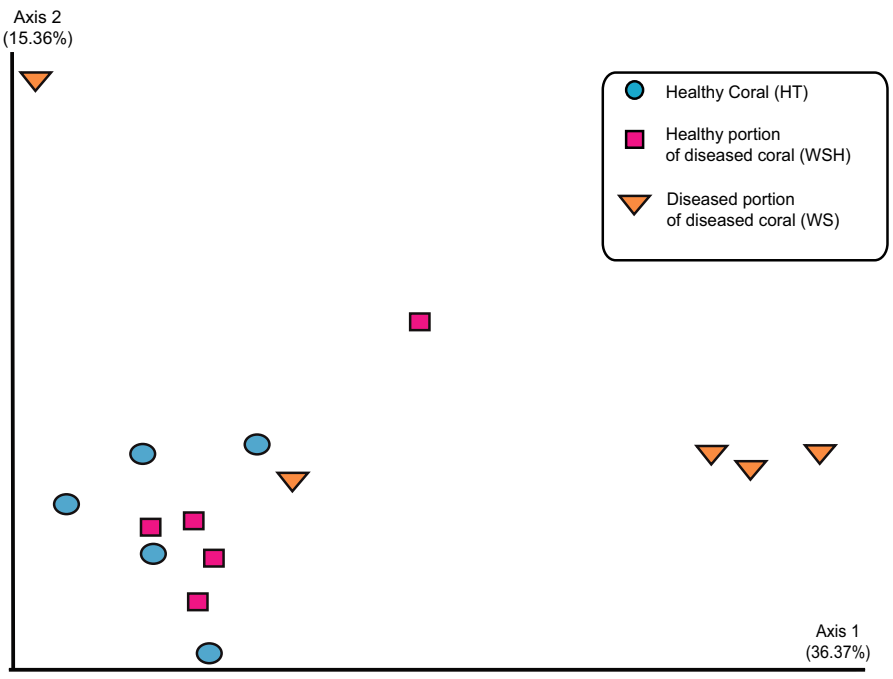

FIGURE 5 Principal coordinate analysis (PCoA) ordination of Weighted UniFrac beta-diversity distances among coral microbial communities assessed using the V4 region of the 16S rDNA. Colours of labels indicate type of disease sample: orange, diseased tissue in diseased colony (WS); pink, healthy tissue in diseased colony (WSH); blue, healthy colony (HT). Overall differences in microbial communities between health states were significant by PERMANOVA, however pairwise comparisons were not significant (Table S3). The outlying point in the upper left is MWS5 (see results for more information). A similar ordination plot using Bray-Curtis dissimilarities is shown in Figure S3

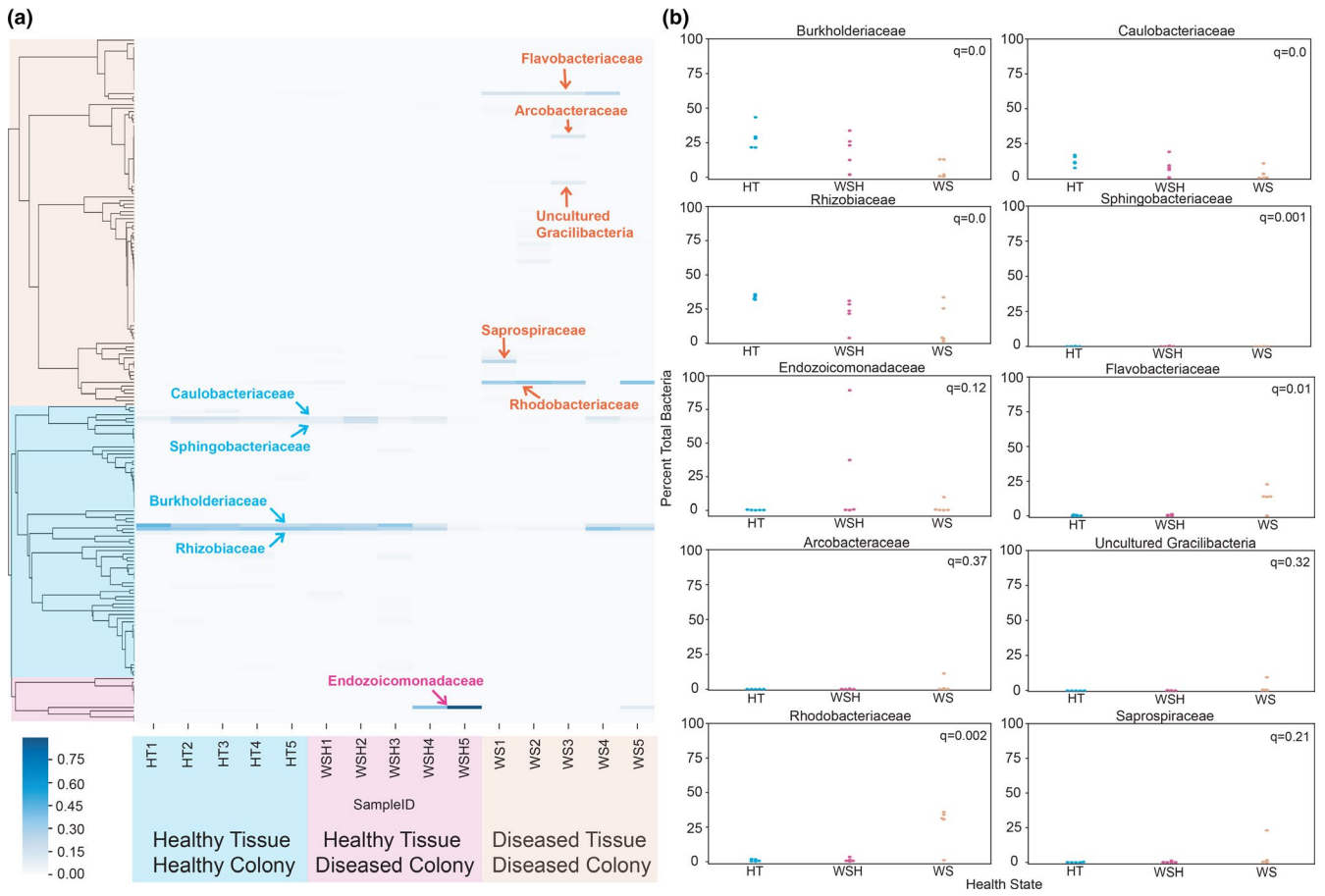

FIGURE 6 (a) Prevalence and distribution of the bacterial families identified in this study ordered by disease state. Named bacterial families are of the top ten overall abundance families. (b) Swarm plots generated for the top 10 overall bacterial families by abundance. Colours in both panels indicate disease state of sample: Blue = HT; Pink = WSH; Orange = WS. *q* values indicate GLMM values for the bacterial family

taxonomic annotations regardless of number of reads is available in Table S4A–D, and was used for statistical analysis. All bacterial communities associated with *M. capitata* samples were composed predominantly of the phylum Proteobacteria (ranging from 38% to 92% relative abundance; Figures S4 and S5; Table S4A). We tested for differences in the relative abundance of Proteobacteria across health states, but did not detect significant differences (GLMM, FDR q = .137). In MWS samples, members of phylum Bacteroidetes were ~11× higher in relative abundance on average than in WSH samples and ~13× higher in relative abundance than in HT samples but this difference was not statistically significant (p = .06; Figures S4 and S5; Table S4A).

We further analysed the Proteobacteria at the class level. Alphaproteobacteria were the predominant bacterial class in almost all samples making up 31%–66% of reads (Figures S6 and S7; Table S4B). The exception to the dominance of Alphaproteobacteria were samples WSH5 and WSH4 which were dominated by Gammaproteobacteria (Figures S6 and S7). To further explore potential changes within the Proteobacteria with cMWS, we used GLMMs to test for changes in the relative abundance of classes of Proteobacteria. Several bacterial classes showed significant differences in relative abundance across disease states (Figures S6 and S7). Betaproteobacteria (GLMM, FDR q = .024) were enriched in apparently healthy tissues (HT and WSH) showing significantly greater relative abundance in HT tissue (GLMM, FDR q = .009) or WSH tissue (GLMM, FDR q = .05) when compared to WS tissues. Conversely, Deltaproteobacteria (GLMM, FDR q = .027) showed greater abundance in WS tissues when compared to WSH (EMM, FDR q = .032) and HT (EMM, FDR q = .012). We did not find significant differences in Alphaproteobacteria (GLMM, q = .604), Epsilonproteobacteria (GLMM, FDR q = .343), or Gammaproteobacteria (GLMM, FDR q = .164) between health states.

We also analysed differences in relative abundance at the genus level for the most abundant bacteria regardless of taxonomy. In this analysis, we included genera that were among the 10 most abundant in any sample (45 total genera, see Table S4E). The relative abundance of these top 10 bacterial genera ranged from 52% of the sample in HT3 to 93% of the sample in WSH5 (Table S4E). Following control for the false discovery rate, 11 genera showed significant differences in relative abundance between health states (Table S4E).

3.7 | Microbial community comparison to health state and immunity

Analyses using indicspecies and weighted correlation network analysis (WGCNA) were also conducted to elucidate microbial families and genera associated with the three health states (WS, WSH, and HT). The analysis using the indicspecies R package found 14 bacterial families (Table S4F) and 15 genera (Table S4G) to be good indicator taxa for WS tissue. No bacterial families or genera were found to be good indicator taxa for WSH or HT tissues alone. However, families Pseudomonadaceae and Corynebacteriaceae (Table S4E) were found to be good indicator taxa for both WSH and HT. At the family level, Pseudoalteromonadaceae (Table S4F) was a good indicator taxa for WS and WSH tissue while *Ruegeria*, *Winogradskyella*, and *Pseudoalteromonas* (Table S4G) were found to be good indicator taxa at the genus level for both WS and WSH tissues combined.

Furthermore, the WGCNA analysis was used to find clusters of bacterial families that were correlated in abundance with the five immune parameters. A significant positive correlation (WGCNA, $p = .01$, Figure S2) between bacterial families and tyrosine-type catecholase activity (dopamine) was found from the analysis. A total of 17 families were found to be driving this interaction (Table S4H). None of the other comparisons were found to be significantly correlated (Figure S2; Table S4I). Additionally, there did not appear to be a visible pattern in immune assay substrate used and tissue type (Figure S2A) indicating a high variation in immune response. None of the indicator taxa were identified in the WGCNA analysis.

4 | DISCUSSION

Bacterial and algal symbiont community compositions have been previously studied for some coral diseases (Cárdenas et al., 2012; Cervino et al., 2004; Closek et al., 2014; Cróquer et al., 2013; Kellogg et al., 2013, 2014; Sato et al., 2010; Sunagawa et al., 2009) with only a few studies examining the combined effect of coral-associated microbial community and immune response to disease (Closek et al., 2014; Daniels et al., 2015). In this study we analysed microbial dynamics and immunocompetence to better understand how *M. capitata* responds to cMWS as well as how the disease affects the microbial community of the coral. More importantly, we can begin to understand how the microbiome may influence or interact with the immune system of the host.

4.1 | Immune response

Total potential PO activity was used as a proxy for immunocompetence in the melanin synthesis pathway of diseased and healthy *M. capitata*. These assays have previously been used in a variety of studies to measure immunocompetence in corals (D'Angelo et al., 2012; Palmer, Bythell, et al., 2011; Pinzon et al., 2014; Pollock et al., 2019; Sheridan et al., 2014; van de Water et al., 2016; van de Water et al., 2015; van de Water, Leggat, et al., 2015; van de Water, Ainsworth, et al., 2015). We found that enzymatic activity of the studied components of the melanin synthesis pathway varied between disease states as well as between the melanin pathway constituents. Using multiple substrates to measure immunocompetence in *M. capitata* allowed for a better understanding of how the melanin synthesis pathway responds to disease. In WS infected tissue, we found low cresolase and catecholase (L-DOPA and dopamine) enzymatic activities throughout the melanin synthesis pathway. This result indicates suppression of this combined pathway during disease and would be expected to occur if an organism has succumbed to disease. On the other hand, the healthy portions of diseased colonies showed increased activity of all three enzymes indicating that these tissues exhibited an immune response and were actively working to combat the WS infection. In healthy colonies we found high enzymatic activity on the first steps of the melanin synthesis pathway but low activity in the last step (dopamine synthesis) that ultimately leads to melanin formation. This "front loading" (Barshis et al., 2013) suggests that this arm of the melanin synthesis pathway is normally primed for future immunological activity in healthy individuals.

Our results are consistent with previous studies that found lower PO activity in infected tissues (Mydlarz et al., 2008; Palmer, Bythell, et al., 2011) and high PO activity in corals showing resistance to disease (Palmer et al., 2010; van de Water et al., 2015).

Assays for a third substrate for catecholase activity, 4-methylcatechol, did not show differences in enzymatic activity between tissue types. In the honey bee, *Apis mellifera*, lower levels of the substrate 4-methylcatechol resulted in greater susceptibility to the bacterial pathogen, *Paenibacillus*, (Chan et al., 2009). This substrate was also associated with immunity inhibition by *Photorhabdus* in the tobacco hornworm, *Manduca sexta* (Eleftherianos et al., 2006). The consistent enzymatic activities of catecholase when 4-methylcatechol was used as the substrate suggests that both healthy and unhealthy tissues are under stress and are showing immunocompetence or that it is not a component of the immune response of *M. capitata* to cMWS.

Laccase-type activity has previously been found in Pacific anthozoans and was hypothesized to be involved in disease resistance in corals (Palmer & Traylor-Knowles, 2012). In this study, WSH and WS tissues showed greater laccase-type activity when compared to HT tissue indicating that laccase is involved in combating cMWS in *M. capitata*. The utility of laccase-type activity in innate immunity has been identified in crayfish and Drosophila where this enzyme participates in the formation of a hardened capsule around the invading pathogen (Barrett, 1987; Cárdenas & Dankert, 2000). Additionally, laccase-type activity caused greater inhibition of pathogenic bacteria in *Crassostrea gigas* hemocyte lysate than catecholase activity (Luna-Acosta et al., 2011).

4.2 | Microbial analysis

We found that *M. capitata* had twice the bacterial richness in diseased tissues when compared to healthy tissues (mean 415.6 vs.

176.8 unique ASVs per sample), but no differences were found in community evenness between tissue types. Higher bacterial richness in diseased tissue was also observed by other studies such as in *Orbicella faveolata* infected with white plague disease (Sunagawa et al., 2009) and in *Pseudodiploria strigosa*, *O. annularis*, and *Colpophyllia natans* infected with black band disease (Cooney et al., 2002). Other white syndrome studies have also found that diseased coral tissue possess greater microbial diversity than healthy tissue in *Turbinaria mesenterina* and Australian acroporid corals (Godwin et al., 2012; Pollock et al., 2017).

It is postulated that corals harbour a specific bacterial community and that during disease this association breaks down and falls into disequilibrium. As a result of the bacterial core community breakdown, opportunistic bacteria inhabit the coral, increasing the bacterial diversity in diseased tissue (Costello et al., 2012; Rohwer et al., 2001). Could the outlying samples in cMWS microbiomes represent Anna Karenina Principle effects (AKP effects; Zaneveld et al., 2017)? Our analysis did not find a significant difference in dispersion between health states overall. There were some hints that dispersion in Bray-Curtis dissimilarities may differ between health and cMWS colonies - which would indicate AKP effects, but these differences were not significant after correction for multiple comparisons. Future cMWS studies might consider testing for increased dispersion in cMWS tissues relative to healthy *Montipora* as a prior hypothesis to address this issue with improved statistical power. We identified indicator families that were present only in WS tissue but no families were found to be good indicators for WSH or HT samples. In our study we found that WSH and HT tissues were similar to one another in microbiome richness (Figure 4a), indicating that the effects of cMWS are very localized and restricted to the diseased tissue portion of the colony. In this way, the coral host may be capable of quarantining the pathogen or pathogens responsible for disease, thereby slowing progression of the disease.

Our results differ from a previous study on *M. capitata* looking at the fast, progressive form of MWS (acute MWS or aMWS) which discovered that the microbial community diversity and species richness were lower in diseased samples when compared to healthy tissue of diseased and healthy colonies (Beurmann et al., 2018). This pattern has also been found in colonies of *O. faveollata* experiencing yellow band disease, the "healthy" portions of the diseased colonies showed the greatest microbial diversity (Closek et al., 2014). In *A. millepora*, corals that would develop WS had lower bacterial diversity and greater community heterogeneity between colonies compared to healthy corals (Pollock et al., 2019).

In *M. capitata*, bacterial community sequencing found predominantly members of the phylum Proteobacteria regardless of health state. This finding is in line with other coral disease studies (Beurmann et al., 2018; Shore-Maggio et al., 2015; Sunagawa et al., 2010). Within the phylum Proteobacteria, the dominant class in all health states was Alphaproteobacteria. This finding differs from previous work done on healthy *M. capitata* in the same location (Kāne'ohe Bay) where Gammaproteobacteria were the dominant proteobacteria (Shore-Maggio et al., 2015). The contrasting results may be due to differences in the collection sites and/or time of collection since seasonal differences have been shown to shift coral microbial communities (Sharp et al., 2017).

Within the phylum Proteobacteria, Betaproteobacteria were found in greater abundance in HT and WSH tissue when compared to WS tissue. Members of this class have been found across coral genera (Dunphy et al., 2019) and are known to play a key role in nutrient cycling and promote plant growth by synthesizing phytohormones and vitamins (Gyaneshwar et al., 2011). A second class of Proteobacteria, Deltaproteobacteria, was found in greater abundance in diseased tissue than in both healthy tissue types. This bacterial class contains predatory bacteria such as *Halobacteriovorax* which was found to be a good indicator taxa for WS infected tissues in *M. capitata*. *Halobacteriovorax* is common in coral mucus (Welsh et al., 2016), feeds on *Vibrio* spp. (and probably other microbes), and can protect corals against Vibrio-induced disease and microbiome disruption (Welsh et al., 2017).

At the genus level, no differences were observed for *Vibrio* spp. between healthy and diseased states. This is surprising as *Vibrio owensii*, has been identified as a possible causative agent of cMWS (Ushijima et al., 2012). A previous study using *Vibrio corallilyticus* to induce tissue loss showed that *Vibrio* pathogens may be lost after initial infection (Welsh et al., 2017) and may not be detected in microbiome surveys even if they caused the disease (Welsh et al., 2017). Our results do not exclude the possibility that *V. owensii* is involved at some stage of pathogenesis, but do argue that it is not a persistent and common member of the microbiome of corals with visible cMWS. It is likely that some members of *Vibrio* spp. are part of the healthy microbial community in *M. capitata* but may shift to more pathogenic *Vibrio* spp. communities during disease progression or when environmental conditions change (example *V. coralliilyticus*; Ben-Haim & Rosenberg, 2002) (Tout et al., 2015). Future metagenomic studies on cMWS during early infection and disease progression could elucidate which bacterial members are involved and contributing most to disease outbreaks and progression.

The high abundance of *Pseudoalteromonas* spp. in diseased colonies (WS and WSH tissue types) and its identification as a good indicator taxa for these two tissue types shows that this taxon may also be important in cMWS. *Pseudoalteromonas piratica* is an abundant member of the culturable bacterial community associated with aMWS and this bacterium has been shown to cause a switch from cMWS to aMWS (Beurmann et al., 2017). Additionally, it is possible that cMWS is not caused by a specific pathogen but rather a collection of generic symptoms that can be elicited by a number of opportunistic pathogens when the immune system of the organism is compromised (Krediet, Ritchie, Alagely, et al., 2013; Lesser et al., 2007).

Bdellovibrio spp. sequences were found only in white syndrome infected tissue and were also shown to be a good indicator taxa for WS. Interestingly, samples that lacked *Bdellovibrio* showed a higher presence of *Pseudomonas* spp. sequences which were more abundant in HT and WSH than WS tissue and were found to be good indicator taxa for the two tissue types. *Bdellovibrio* spp. has been

shown to consume *Pseudomonas aeruginosa* in humans with cystic fibrosis (Iebba et al., 2014) which suggests that *Bdellovibrio* spp. may negatively affect *Pseudomonas* spp. in *M. capitata* with cMWS. *Pseudomonas* spp. are also known to be beneficial to their host. In plants, *Pseudomonas* spp. have been associated with growth, waste degradation, toxic chemical remediation and reduction of disease severity (Novik et al., 2015). In the marine environment, *Pseudomonas* spp. have been involved in coral nutrient cycling (Zhang et al., 2016) and have been shown to produce melanin (Novik et al., 2015). The greater abundance of *Pseudomonas* spp. in healthy coral tissue of *M. capitata* could support nutrient recycling and the production of melanin to keep the coral healthy.

In HT and WSH tissue types, *Rhizobium* spp. and *Burkholderia* spp. accounted for 52%–70% of the bacterial species present in all but two samples. These two bacterial species are probably involved in nitrogen fixation (Krediet, Ritchie, Paul, et al., 2013; Lema et al., 2012) and oxidative recycling of nitrogen-rich metabolic waste (Van Borm et al., 2002) in *M. capitata*. The only two exceptions were WSH4 and WSH5 where the dominant bacterial species was *Endozoicomonas* spp. and made up 51%–80% of the sample composition.

Rhodobacteraceae and Flavobacteriaceae were found in greater abundances in WS tissue when compared to WSH and HT. Both of these families have been previously implicated in coral disease and have been identified as opportunistic pathogens (Sunagawa et al., 2009). Increased prevalence of Rhodobacteraceae was found in diseased corals, *Pavona duerdeni* and *Porites lutea* with white plague disease (Roder et al., 2014). *Flavobacteria* was isolated from a disease outbreak in hatchery reared Chinook salmon, *Onchoryhnchus tshawystscha* (Chen et al., 2017) and have been associated with white band disease in the corals *Acropora palmata* and *A. cervicornis* (Gignoux-Wolfsohn & Vollmer, 2015).

4.3 | Immune and microbiome response during cMWS

Coral samples with lower microbial diversity showed higher enzymatic activity of cresolase and catecholase (using L-DOPA) activities which are the initial components in the proPPO activity pathway. In contrast to our study, Pollock et al. (2019) found a reduction in both bacterial diversity and PO activity in corals that would become infected with WS. Pollock et al. (2019) concluded that high diversity in the microbial community may lead to high functional redundancy which can help to minimize the environmental impacts on coral health. The results of these studies show that bacterial communities can influence coral health in different ways, highlighting the need for more studies that look into the combined effects of microbial communities and the immune system.

A total of 17 bacterial families were found to be associated with catecholase enzymatic activity (measured using dopamine as substrate). Members of several of these families, including Staphylococcaceae, Enterococcaceae, and Microbacteriaceae, have previously been shown to be associated with catecholase activity. Increased abundance of *Staphylococcus epidermis* and high catecholase (using dopamine as a substrate) activity have been shown to accelerate wound healing in mice (Luqman et al., 2020) and could be acting similarly in *M. capitata*. Additionally, decreases in PO activity reduced the abundance of members of the bacterial family Enterococcaceae in the insect *Rhodnius prolixus*, though Microbacteriaceae relative abundance remained the same (Vieira et al., 2015).

5 | CONCLUSIONS

We found that during cMWS there are localized changes in microbiome and immune response in the affected tissue area of *M. capitata*. In contrast to previous studies, *Vibrio* spp. was not associated with diseased tissues. However, *Pseudoalteromonas* sp. were found to be significantly enriched in cMWS tissue. Our results show the need for studying multiple enzymes in the melanin synthesis pathway to gain a better understanding of how the coral immune system responds to pathogens. In WS tissues, cresolase (L-tyrosine) and catecholase (L-DOPA and dopamine) displayed low enzymatic activity, an indication that these tissues have succumbed to disease. On the other hand, WSH tissues showed increased activity in the three previously mentioned enzymes; indicating an ongoing immune response. HT tissues demonstrated "front loading" of an immune response with increased cresolase and catecholase (L-DOPA) activity. Laccase-type activity was higher in both WS and WSH tissues when compared to HT indicating that it is probably involved in the immune response of *M. capitata*. Higher activities of catecholase (L-DOPA) and cresolase (L-tyrosine) were associated with lower microbial richness. This study highlights the importance of examining microbial and immune responses simultaneously to gain a holistic insight into how coral diseases affect the coral holobiont and how the host may moderate microbial interactions, confine and kill pathogens and manage chronic perturbations.

ACKNOWLEDGEMENTS

We would like to thank Dr Ruth D. Gates and the entire Gates Laboratory for assistance and use of their laboratory during our time in Hawai'i. We are grateful to Brenner Wakayama for assistance with field collections. We would like to thank Jeremy Axworthy, Eileen Bates, Cindy Lewis, and Patricia Waikel for comments on the manuscript. This research was funded by a Sloan Research Fellowship and an NSF-IOS grant (#1655682) awarded to JLPG.

AUTHOR CONTRIBUTIONS

Jaqueline L. Padilla-Gamiño and Tanya Brown designed the research. Tanya Brown performed the research. Jaqueline L. Padilla-Gamiño, Tanya Brown, Jesse R. Zaneveld and Dylan Sonett contributed new reagents or analytical tools. Jaqueline L. Padilla-Gamiño, Tanya Brown, Jesse R. Zaneveld and Dylan Sonett analysed the data and wrote the manuscript.

DATA AVAILABILITY STATEMENT

All processing steps for quality control of 16S rRNA analysis are available on GitHub (https://github.com/sonettd/MWS). 16S rRNA sequences have been deposited in Genebank under SRA data: PRJNA662110.

ORCID

Tanya Brown https://orcid.org/0000-0003-0103-7510
Dylan Sonett http://orcid.org/0000-0001-6821-4695
Jesse R. Zaneveld https://orcid.org/0000-0002-9823-810X

REFERENCES

Aeby, G. S. (2006). Baseline levels of coral disease in the Northwestern Hawaiian Islands. *Atoll Research Bulletin*, *543*, 471–488.

Aeby, G. S., Callahan, S., Cox, E. F., Runyon, C., Smith, A., Stanton, F. G., Ushijima, B., & Work, T. M. (2016). Emerging coral diseases in Kane'ohe Bay, O'ahu, Hawai'i (USA): Two major disease outbreaks of acute *Montipora* white syndrome. *Diseases of Aquatic Organisms*, *119*(3), 189–198. https://doi.org/10.3354/dao02996

Aeby, G. S., Ross, M., Williams, G. J., Lewis, T. D., & Work, T. M. (2010). Disease dynamics of *Montipora* white syndrome within Kaneohe Bay, Oahu, Hawaii: Distribution, seasonality, virulence, and transmissibility. *Diseases of Aquatic Organisms*, *91*(1), 1–8. https://doi.org/10.3354/dao02247

Anderson, M. J. (2001). A new method for non-parametric multivariate analysis of variance. *Austral Ecology*, *26*(1), 32–46.

Arakane, Y., Muthukrishnan, S., Beeman, R. W., Kanost, M. R., & Kramer, K. J. (2005). Laccase 2 is the phenoloxidase gene required for beetle cuticle tanning. *Proceedings of the National Academy of Sciences of the United States of America*, *102*(32), 11337–11342.

Bak, R. P. M., Joenje, M., de Jong, I., Lambrechts, D. Y. M., & Nieuwland, G. (1998). Bacterial suspension feeding by coral reef benthic organisms. *Marine Ecology Progress Series*, *175*, 285–288. https://doi.org/10.3354/meps175285

Barrett, F. M. (1987). Characterization of phenoloxidases from larval cuticle of *Sarcophaga bullata* and a comparison with cuticular enzymes from other species. *Canadian Journal of Zoology*, *65*(5), 1158–1166.

Barshis, D. J., Ladner, J. T., Oliver, T. A., Seneca, F. O., Traylor-Knowles, N., & Palumbi, S. R. (2013). Genomic basis for coral resilience to climate change. *Proceedings of the National Academy of Sciences of the United States of America*, *110*(4), 1387–1392. https://doi.org/10.1073/pnas.1210224110

Bengtsson-Palme, J., Hartmann, M., Eriksson, K. M., Pal, C., Thorell, K., Larsson, D. G. J., & Nilsson, R. H. (2015). METAXA2: Improved identification and taxonomic classification of small and large subunit rRNA in metagenomic data. *Molecular Ecology Resources*, *15*(6), 1403–1414.

Ben-Haim, Y., & Rosenberg, E. (2002). A novel *Vibrio* sp. pathogen of the coral *Pocillopora damicornis*. *Marine Biology*, *141*(1), 47–55.

Bentis, C. J., Kaufman, L., & Golubic, S. (2000). Endolithic fungi in reef-building corals (Order: Scleractinia) are common, cosmopolitan, and potentially pathogenic. *The Biological Bulletin*, *198*(2), 254–260.

Beurmann, S., Ushijima, B., Svoboda, C. M., Videau, P., Smith, A. M., Donachie, S. P., Aeby, G. S., & Callahan, S. M. (2017). *Pseudoalteromonas piratica* sp nov., a budding, prosthecate bacterium from diseased *Montipora capitata*, and emended description of the genus *Pseudoalteromonas*. *International Journal of Systematic and Evolutionary Microbiology*, *67*(8), 2683–2688. https://doi.org/10.1099/ijsem.0.001995

Beurmann, S., Ushijima, B., Videau, P., Svoboda, C. M., Chatterjee, A., Aeby, G. S., & Callahan, S. M. (2018). Dynamics of acute *Montipora* white syndrome: Bacterial communities of healthy and diseased *M. capitata* colonies during and after a disease outbreak. *Microbiology*, *164*(10), 1240–1253.

Bolyen, E., Rideout, J. R., Dillon, M. R., Bokulich, N. A., Abnet, C. C., Al-Ghalith, G. A., Alexander, H., Alm, E. J., Arumugam, M., Asnicar, F., Bai, Y., Bisanz, J. E., Bittinger, K., Brejnrod, A., Brislawn, C. J., Brown, C. T., Callahan, B. J., Caraballo-Rodríguez, A. M., Chase, J., … Caporaso, J. G. (2019). Reproducible, interactive, scalable and extensible microbiome data science using QIIME 2. *Nature Biotechnology*, *37*(8), 852–857.

Bourne, D. G., Morrow, K. M., & Webster, N. S. (2016). Insights into the coral microbiome: underpinning the health and resilience of reef ecosystems. *Annual Review of Microbiology*, *70*, 317–340.

Bradford, M. M. (1976). A rapid and sensitive method for the quantitation of microgram quantities of protein utilizing the principle of protein-dye binding. *Analytical Biochemistry*, *72*(1–2), 248–254.

Bruno, J. F., Selig, E. R., Casey, K. S., Page, C. A., Willis, B. L., Harvell, C. D., Sweatman, H., & Melendy, A. M. (2007). Thermal stress and coral cover as drivers of coral disease outbreaks. *PLOS Biology*, *5*(6), 1220–1227. https://doi.org/10.1371/journal.pbio.0050124

De Caceres, M., Jansen, F., & De Caceres, M. M. (2016). *Package 'indicspecies'*.

Callahan, B. J., McMurdie, P. J., Rosen, M. J., Han, A. W., Johnson, A. J. A., & Holmes, S. P. (2016). DADA2: High-resolution sample inference from Illumina amplicon data. *Nature Methods*, *13*(7), 581.

Caporaso, J. G., Lauber, C. L., Walters, W. A., Berg-Lyons, D., Lozupone, C. A., Turnbaugh, P. J., Fierer, N., & Knight, R. (2011). Global patterns of 16S rRNA diversity at a depth of millions of sequences per sample. *Proceedings of the National Academy of Sciences of the United States of America*, *108*, 4516–4522. https://doi.org/10.1073/pnas.1000080107

Cárdenas, A., Rodriguez, L. M., Pizarro, V., Cadavid, L. F., & Arévalo-Ferro, C. (2012). Shifts in bacterial communities of two Caribbean reef-building coral species affected by white plague disease. *The ISME Journal*, *6*(3), 502–512.

Cárdenas, W., & Dankert, J. R. (2000). Cresolase, catecholase and laccase activities in haemocytes of the red swamp crayfish. *Fish & Shellfish Immunology*, *10*(1), 33–46.

Cerenius, L., Lee, B. L., & Söderhäll, K. (2008). The proPO-system: pros and cons for its role in invertebrate immunity. *Trends in Immunology*, *29*(6), 263–271.

Cervino, J. M., Hayes, R. L., Polson, S. W., Polson, S. C., Goreau, T. J., Martinez, R. J., & Smith, G. W. (2004). Relationship of *Vibrio* species infection and elevated temperatures to yellow blotch/band disease in Caribbean corals. *Applied and Environmental Microbiology*, *70*(11), 6855–6864. https://doi.org/10.1128/aem.70.11.6855-6864.2004

Chan, Q. W., Melathopoulos, A. P., Pernal, S. F., & Foster, L. J. (2009). The innate immune and systemic response in honey bees to a bacterial pathogen, *Paenibacillus larvae*. *BMC Genomics*, *10*(1), 387.

Chen, S., Blom, J., Loch, T. P., Faisal, M., & Walker, E. D. (2017). The emerging fish pathogen *Flavobacterium spartansii* isolated from chinook salmon: Comparative genome analysis and molecular manipulation. *Frontiers in Microbiology*, *8*, 2339.

Closek, C. J., Sunagawa, S., DeSalvo, M. K., Piceno, Y. M., DeSantis, T. Z., Brodie, E. L., Weber, M. X., Voolstra, C. R., Andersen, G. L., & Medina, M. (2014). Coral transcriptome and bacterial community profiles reveal distinct Yellow Band Disease states in *Orbicella faveolata*. *ISME Journal*, *8*(12), 2411–2422. https://doi.org/10.1038/ismej.2014.85

Connell, J. H. (1978). Diversity in tropical rain forests and coral reefs. *Science*, *199*(4335), 1302–1310.

Cooney, R. P., Pantos, O., Le Tissier, M. D. A., Barer, M. R., O'Donnell, A. G., & Bythell, J. C. (2002). Characterization of the bacterial consortium associated with black band disease in coral using molecular

microbiological techniques. *Environmental Microbiology*, *4*(7), 401–413. https://doi.org/10.1046/j.1462-2920.2002.00308.x

Costello, E. K., Stagaman, K., Dethlefsen, L., Bohannan, B. J. M., & Relman, D. A. (2012). The application of ecological theory toward an understanding of the human microbiome. *Science*, *336*(6086), 1255–1262. https://doi.org/10.1126/science.1224203

Cróquer, A., Bastidas, C., Elliott, A., & Sweet, M. (2013). Bacterial assemblages shifts from healthy to yellow band disease states in the dominant reef coral *Montastraea faveolata*. *Environmental Microbiology Reports*, *5*(1), 90–96.

D'Angelo, C., Smith, E. G., Oswald, F., Burt, J., Tchernov, D., & Wiedenmann, J. (2012). Locally accelerated growth is part of the innate immune response and repair mechanisms in reef-building corals as detected by green fluorescent protein (GFP)-like pigments. *Coral Reefs*, *31*(4), 1045–1056. https://doi.org/10.1007/s00338-012-0926-8

Daniels, C. A., Baumgarten, S., Yum, L. K., Michell, C. T., Bayer, T., Arif, C., Roder, C., Weil, E., & Voolstra, C. R. (2015). Metatranscriptome analysis of the reef-building coral *Orbicella faveolata* indicates holobiont response to coral disease. *Frontiers in Marine Science*, *2*, 62.

DeSantis, T. Z., Hugenholtz, P., Larsen, N., Rojas, M., Brodie, E. L., Keller, K., Huber, T., Dalevi, D., Hu, P., & Andersen, G. L. (2006). Greengenes, a chimera-checked 16S rRNA gene database and workbench compatible with ARB. *Applied and Environmental Microbiology*, *72*(7), 5069–5072. https://doi.org/10.1128/aem.03006-05

Dunphy, C. M., Gouhier, T. C., Chu, N. D., & Vollmer, S. V. (2019). Structure and stability of the coral microbiome in space and time. *Scientific Reports*, *9*(1), 1–13.

Eleftherianos, I., Millichap, P. J., ffrench-Constant, R. H., & Reynolds, S. E. (2006). RNAi suppression of recognition protein mediated immune responses in the tobacco hornworm *Manduca sexta* causes increased susceptibility to the insect pathogen *Photorhabdus*. *Developmental & Comparative Immunology*, *30*(12), 1099–1107.

Ferrier-Pages, C., Godinot, C., D'Angelo, C., Wiedenmann, J., & Grover, R. (2016). Phosphorus metabolism of reef organisms with algal symbionts. *Ecological Monographs*, *86*(3), 262–277.

Forsman, Z. H., Concepcion, G. T., Haverkort, R. D., Shaw, R. W., Maragos, J. E., & Toonen, R. J. (2010). Ecomorph or endangered coral? DNA and microstructure reveal Hawaiian species complexes: *Montipora dilatata/flabellata/turgescens* & *M. patula*/verrilli. *PLoS One*, *5*(12), e15021.

Friedlander, A., Aeby, G., Brainard, R., Brown, E., Chaston, K., Clark, A., … Williams, I. (2008). The state of coral reef ecosystems of the main Hawaiian Islands. In J.E. Waddell & A.M. Clarke *The state of coral reef ecosystems of the United States and Pacific freely associated states* (vol. *17*). NOAA/National Centers of Coastal Ocean Science.

Gignoux-Wolfsohn, S. A., & Vollmer, S. V. (2015). Identification of candidate coral pathogens on white band disease-infected staghorn coral. *PLoS One*, *10*(8), e0134416.

Godwin, S., Bent, E., Borneman, J., & Pereg, L. (2012). The role of coral-associated bacterial communities in Australian subtropical white syndrome of *Turbinaria mesenterina*. *PLoS One*, *7*(9), e44243. https://doi.org/10.1371/journal.pone.0044243

Gyaneshwar, P., Hirsch, A. M., Moulin, L., Chen, W.-M., Elliott, G. N., Bontemps, C., Estrada-de los Santos, P., Gross, E., dos Reis, F. B., Sprent, J. I., Young, J. P. W., & James, E. K. (2011). Legume-nodulating betaproteobacteria: diversity, host range, and future prospects. *Molecular Plant-Microbe Interactions*, *24*(11), 1276–1288.

Harvell, C. D., & Lamb, J. B. (2020). Disease outbreaks can threaten marine biodiversity. Donald C. Behringer Brian R. Silliman & Kevin D. Lafferty (Eds.), *Marine Disease Ecology*, 141–158. Oxford Scholorship. https://doi.org/10.1093/oso/9780198821632.003.0008.

Harvell, C. D., Mitchell, C. E., Ward, J. R., Altizer, S., Dobson, A. P., Ostfeld, R. S., & Samuel, M. D. (2002). Ecology - climate warming and disease risks for terrestrial and marine biota. *Science*, *296*(5576), 2158–2162. https://doi.org/10.1126/science.1063699

Iebba, V., Totino, V., Santangelo, F., Gagliardi, A., Ciotoli, L., Virga, A., Ambrosi, C., Pompili, M., De Biase, R. V., Selan, L., Artini, M., Pantanella, F., Mura, F., Passariello, C., Nicoletti, M., Nencioni, L., Trancassini, M., Quattrucci, S., & Schippa, S. (2014). *Bdellovibrio bacteriovorus* directly attacks *Pseudomonas aeruginosa* and *Staphylococcus aureus* cystic fibrosis isolates. *Frontiers in Microbiology*, *5*, 280.

Irving, P., Troxler, L., & Hetru, C. (2004). Is innate enough? The innate immune response in Drosophila. *Comptes Rendus Biologies*, *327*(6), 557–570. https://doi.org/10.1016/j.crvi.2004.03.007

Kellogg, C. A., Piceno, Y. M., Tom, L. M., DeSantis, T. Z., Gray, M. A., & Andersen, G. L. (2014). Comparing bacterial community composition of healthy and dark spot-affected *Siderastrea siderea* in Florida and the Caribbean. *PLoS One*, *9*(10), e108767.

Kellogg, C. A., Piceno, Y. M., Tom, L. M., DeSantis, T. Z., Gray, M. A., Zawada, D. G., & Andersen, G. L. (2013). Comparing bacterial community composition between healthy and white plague-like disease states in *Orbicella annularis* using PhyloChip (TM) G3 microarrays. *PLoS One*, *8*(11), https://doi.org/10.1371/journal.pone.0079801

Kimes, N. E., Van Nostrand, J. D., Weil, E., Zhou, J. Z., & Morris, P. J. (2010). Microbial functional structure of Montastraea faveolata, an important Caribbean reef-building coral, differs between healthy and yellow-band diseased colonies. *Environmental Microbiology*, *12*(2), 541–556. https://doi.org/10.1111/j.1462-2920.2009.02113.x

Kline, D. I., & Vollmer, S. V. (2011). White Band Disease (type I) of endangered Caribbean acroporid corals is caused by pathogenic bacteria. *Scientific Reports*, *1*, 7.

Krediet, C. J., Ritchie, K. B., Alagely, A., & Teplitski, M. (2013). Members of native coral microbiota inhibit glycosidases and thwart colonization of coral mucus by an opportunistic pathogen. *The ISME Journal*, *7*(5), 980–990.

Krediet, C. J., Ritchie, K. B., Paul, V. J., & Teplitski, M. (2013). Coral-associated micro-organisms and their roles in promoting coral health and thwarting diseases. *Proceedings of the Royal Society B: Biological Sciences*, *280*(1755), 20122328.

Lafferty, K. D., Porter, J. W., & Ford, S. E. (2004). Are diseases increasing in the ocean? *Annual Review of Ecology, Evolution and Systematics*, *35*, 31–54.

Langfelder, P., & Horvath, S. (2008). WGCNA: An R package for weighted correlation network analysis. *BMC Bioinformatics*, *9*(1), 559.

Lema, K. A., Willis, B. L., & Bourne, D. G. (2012). Corals form characteristic associations with symbiotic nitrogen-fixing bacteria. *Applied and Environmental Microbiology*, *78*(9), 3136–3144.

Lesser, M. P., Bythell, J. C., Gates, R. D., Johnstone, R. W., & Hoegh-Guldberg, O. (2007). Are infectious diseases really killing corals? Alternative interpretations of the experimental and ecological data. *Journal of Experimental Marine Biology and Ecology*, *346*(1–2), 36–44.

Luna-Acosta, A., Saulnier, D., Pommier, M., Haffner, P., De Decker, S., Renault, T., & Thomas-Guyon, H. (2011). First evidence of a potential antibacterial activity involving a laccase-type enzyme of the phenoloxidase system in Pacific oyster *Crassostrea gigas* haemocytes. *Fish & Shellfish Immunology*, *31*(6), 795–800.

Luqman, A., Muttaqin, M. Z., Yulaipi, S., Ebner, P., Matsuo, M., Zabel, S., Tribelli, P. M., Nieselt, K., Hidayati, D., & Götz, F. (2020). Trace amines produced by skin bacteria accelerate wound healing in mice. *Communications Biology*, *3*(1), 1–10.

Mydlarz, L. D., Couch, C. S., Weil, E., Smith, G., & Harvell, C. D. (2009). Immune defenses of healthy, bleached and diseased *Montastraea faveolata* during a natural bleaching event. *Diseases of Aquatic Organisms*, *87*(1–2), 67–78. https://doi.org/10.3354/dao02088

Mydlarz, L. D., Holthouse, S. F., Peters, E. C., & Harvell, C. D. (2008). Cellular responses in sea fan corals: granular amoebocytes react to pathogen and climate stressors. *PLoS One*, *3*(3), e1811.

Mydlarz, L. D., McGinty, E. S., & Harvell, C. D. (2009). What are the physiological and immunological responses of coral to climate warming and disease? *Journal of Experimental Biology*, *213*(6), 934–945. https://doi.org/10.1242/jeb.037580

Mydlarz, L. D., & Palmer, C. V. (2011). The presence of multiple phenoloxidases in Caribbean reef-building corals. *Comparative Biochemistry and Physiology a-Molecular & Integrative Physiology*, *159*(4), 372–378. https://doi.org/10.1016/j.cbpa.2011.03.029

Nappi, A. J., & Ottaviani, E. (2000). Cytotoxicity and cytotoxic molecules in invertebrates. *BioEssays*, *22*(5), 469–480.10.1002/(sici)1521-1878(200005)22:5<469:Aid-bies9>3.3.Co;2-w

Novik, G., Savich, V., & Kiseleva, E. (2015). An insight into beneficial *Pseudomonas* bacteria. In Mohammad Manjur Shah *Microbiology in agriculture and human health* (pp. 73–105). Yusuf Maitama Sule University. https://doi.org/10.5772/59645.

Odum, H. T., & Odum, E. P. (1955). Trophic structure and productivity of a windward coral reef community on Eniwetok Atoll. *Ecological Monographs*, *25*(3), 291–320.

Palmer, C. V., Bythell, J. C., & Willis, B. L. (2010). Levels of immunity parameters underpin bleaching and disease susceptibility of reef corals. *FASEB Journal*, *24*(6), 1935–1946. https://doi.org/10.1096/fj.09-152447

Palmer, C. V., Bythell, J. C., & Willis, B. L. (2011). A comparative study of phenoloxidase activity in diseased and bleached colonies of the coral *Acropora millepora*. *Developmental and Comparative Immunology*, *35*(10), 1096–1099. https://doi.org/10.1016/j.dci.2011.04.001

Palmer, C., Bythell, J. C., & Willis, B. (2012). Enzyme activity demonstrates multiple pathways of innate immunity in Indo-Pacific anthozoans. *Proceedings of the Royal Society B: Biological Sciences*, *279*(1743), 3879–3887.

Palmer, C. V., & Traylor-Knowles, N. (2012). Towards an integrated network of coral immune mechanisms. *Proceedings of the Royal Society B: Biological Sciences*, *279*(1745), 4106–4114. https://doi.org/10.1098/rspb.2012.1477

Palmer, C. V., Traylor-Knowles, N., Willis, B. L., & Bythell, J. C. (2011). Corals use similar immune cells and wound-healing processes as those of higher organisms. *PLoS One*, *6*(8), e23992. https://doi.org/10.1371/journal.pone.0023992

Peters, E. C. (2015). Diseases of coral reef organisms. In *Coral reefs in the Anthropocene* (pp. 147–178). Springer.

Pinzon, C. J. H., Dornberger, L., Beach-Letendre, J., Weil, E., & Mydlarz, L. D. (2014). The link between immunity and life history traits in scleractinian corals. *PeerJ*, *2*, e628. https://doi.org/10.7717/peerj.628

Plowright, R. K., Sokolow, S. H., Gorman, M. E., Daszak, P., & Foley, J. E. (2008). Causal inference in disease ecology: investigating ecological drivers of disease emergence. *Frontiers in Ecology and the Environment*, *6*(8), 420–429.

Pollock, F. J., Lamb, J. B., van de Water, J. A., Smith, H. A., Schaffelke, B., Willis, B. L., & Bourne, D. G. (2019). Reduced diversity and stability of coral-associated bacterial communities and suppressed immune function precedes disease onset in corals. *Royal Society Open Science*, *6*(6), 190355.

Pollock, F. J., Morris, P. J., Willis, B. L., & Bourne, D. G. (2011). The urgent need for robust coral disease diagnostics. *PLoS Pathogy*, *7*(10), e1002183.

Pollock, F. J., Wada, N., Torda, G., Willis, B. L., & Bourne, D. G. (2017). White syndrome-affected corals have a distinct microbiome at disease lesion fronts. *Applied and Environmental Microbiology*, *83*(2), 16. https://doi.org/10.1128/aem.02799-16

Quast, C., Pruesse, E., Yilmaz, P., Gerken, J., Schweer, T., Yarza, P., Peplies, J., & Glöckner, F. O. (2012). The SILVA ribosomal RNA gene database project: improved data processing and web-based tools. *Nucleic Acids Research*, *41*(D1), D590–D596.

Reaka-Kudla, M. L. (1997). The global biodiversity of coral reefs: a comparison with rain forests. *Biodiversity II: Understanding and Protecting our Biological Resources*, *2*, 551.

Roder, C., Arif, C., Bayer, T., Aranda, M., Daniels, C., Shibl, A., Chavanich, S., & Voolstra, C. R. (2014). Bacterial profiling of White Plague Disease in a comparative coral species framework. *The ISME Journal*, *8*(1), 31–39.

Rognes, T., Flouri, T., Nichols, B., Quince, C., & Mahé, F. (2016). VSEARCH: a versatile open source tool for metagenomics. *PeerJ*, *4*, e2584.

Rohwer, F., Breitbart, M., Jara, J., Azam, F., & Knowlton, N. (2001). Diversity of bacteria associated with the Caribbean coral *Montastraea franksi*. *Coral Reefs*, *20*(1), 85–91.

Rohwer, F., Seguritan, V., Azam, F., & Knowlton, N. (2002). Diversity and distribution of coral-associated bacteria. *Marine Ecology Progress Series*, *243*, 1–10. https://doi.org/10.3354/meps243001

Sato, Y., Willis, B. L., & Bourne, D. G. (2010). Successional changes in bacterial communities during the development of black band disease on the reef coral, *Montipora hispida*. *The ISME Journal*, *4*(2), 203–214.

Schlichter, D., Kampmann, H., & Conrady, S. (1997). Trophic potential and photoecology of endolithic algae living within coral skeletons. *Marine Ecology*, *18*(4), 299–317.

Sharp, K. H., Pratte, Z. A., Kerwin, A. H., Rotjan, R. D., & Stewart, F. J. (2017). Season, but not symbiont state, drives microbiome structure in the temperate coral *Astrangia poculata*. *Microbiome*, *5*(1), 120.

Shashar, N., Cohen, Y., Loya, Y., & Sar, N. (1994). Nitrogen-fixation (acetylene-reduction) in stony corals-evidence for-coral-bacteria interactions. *Marine Ecology Progress Series*, *111*(3), 259–264. https://doi.org/10.3354/meps111259

Sheridan, C., Grosjean, P., Leblud, J., Palmer, C. V., Kushmaro, A., & Eeckhaut, I. (2014). Sedimentation rapidly induces an immune response and depletes energy stores in a hard coral. *Coral Reefs*, *33*(4), 1067–1076. https://doi.org/10.1007/s00338-014-1202-x

Shore-Maggio, A., Runyon, C. M., Ushijima, B., Aeby, G. S., & Callahan, S. M. (2015). Differences in bacterial community structure in two color morphs of the Hawaiian reef coral *Montipora capitata*. *Applied and Environmental Microbiology*, *81*(20), 7312–7318. https://doi.org/10.1128/aem.01935-15

Siboni, N., Ben-Dov, E., Sivan, A., & Kushmaro, A. (2008). Global distribution and diversity of coral-associated Archaea and their possible role in the coral holobiont nitrogen cycle. *Environmental Microbiology*, *10*(11), 2979–2990. https://doi.org/10.1111/j.1462-2920.2008.01718.x

Sorokin, Y. I. (1973). On the feeding of some scleractinian corals with bacteria and dissolved organic matter. *Limnology and Oceanography*, *18*(3), 380–386.

Sunagawa, S., DeSantis, T. Z., Piceno, Y. M., Brodie, E. L., DeSalvo, M. K., Voolstra, C. R., Weil, E., Andersen, G. L., & Medina, M. (2009). Bacterial diversity and White Plague Disease-associated community changes in the Caribbean coral *Montastraea faveolata*. *ISME Journal*, *3*(5), 512–521. https://doi.org/10.1038/ismej.2008.131

Sunagawa, S., Woodley, C. M., & Medina, M. (2010). Threatened Corals Provide Underexplored Microbial Habitats. *PLoS One*, *5*(3), e9554. https://doi.org/10.1371/journal.pone.0009554

Sutherland, K. P., Porter, J. W., & Torres, C. (2004). Disease and immunity in Caribbean and Indo-Pacific zooxanthellate corals. *Marine Ecology Progress Series*, *266*, 273–302. https://doi.org/10.3354/meps266273

Tang, H., Kambris, Z., Lemaitre, B., & Hashimoto, C. (2006). Two proteases defining a melanization cascade in the immune system of *Drosophila*. *Journal of Biological Chemistry*, *281*(38), 28097–28104.

Tout, J., Siboni, N., Messer, L. F., Garren, M., Stocker, R., Webster, N. S., Ralph, P. J., & Seymour, J. R. (2015). Increased seawater temperature increases the abundance and alters the structure of

natural *Vibrio* populations associated with the coral *Pocillopora damicornis*. *Frontiers in Microbiology*, *6*, 432. https://doi.org/10.3389/fmicb.2015.00432

Upton, S. J., & Peters, E. C. (1986). A new and unusual species of coccidium (Apicomplexa: Agamococcidiorida) from Caribbean scleractinian corals. *Journal of Invertebrate Pathology*, *47*(2), 184–193.

Ushijima, B., Smith, A., Aeby, G. S., & Callahan, S. M. (2012). *Vibrio owensii* induces the tissue loss disease *Montipora* white syndrome in the Hawaiian reef coral *Montipora capitata*. *PLoS One*, *7*(10), https://doi.org/10.1371/journal.pone.0046717

Ushijima, B., Videau, P., Burger, A. H., Shore-Maggio, A., Runyon, C. M., Sudek, M., Aeby, G. S., & Callahan, S. M. (2014). *Vibrio coralliilyticus* strain OCN008 Is an etiological agent of acute *Montipora* white syndrome. *Applied and Environmental Microbiology*, *80*(7), 2102–2109. https://doi.org/10.1128/aem.03463-13

Van Borm, S., Buschinger, A., Boomsma, J. J., & Billen, J. (2002). Tetraponera ants have gut symbionts related to nitrogen–fixing root–nodule bacteria. *Proceedings of the Royal Society of London B: Biological Sciences*, *269*(1504), 2023–2027.

van de Water, J. A., Ainsworth, T. D., Leggat, W., Bourne, D. G., Willis, B. L., & Van Oppen, M. J. (2015). The coral immune response facilitates protection against microbes during tissue regeneration. *Molecular Ecology*, *24*(13), 3390–3404.

van de Water, J., Lamb, J. B., Heron, S. F., van Oppen, M. J. H., & Willis, B. L. (2016). Temporal patterns in innate immunity parameters in reef-building corals and linkages with local climatic conditions. *Ecosphere*, *7*(11), e01505. https://doi.org/10.1002/ecs2.1505

van de Water, J., Lamb, J. B., van Oppen, M. J. H., Willis, B. L., & Bourne, D. G. (2015). Comparative immune responses of corals to stressors associated with offshore reef-based tourist platforms. *Conservation Physiology*, *3*, cov032. https://doi.org/10.1093/conphys/cov032

van de Water, J., Leggat, W., Bourne, D. G., van Oppen, M. J. H., Willis, B. L., & Ainsworth, T. D. (2015). Elevated seawater temperatures have a limited impact on the coral immune response following physical damage. *Hydrobiologia*, *759*(1), 201–214. https://doi.org/10.1007/s10750-015-2243-z

Vieira, C. S., Mattos, D. P., Waniek, P. J., Santangelo, J. M., Figueiredo, M. B., Gumiel, M., da Mota, F. F., Castro, D. P., Garcia, E. S., & Azambuja, P. (2015). *Rhodnius prolixus* interaction with *Trypanosoma rangeli*: modulation of the immune system and microbiota population. *Parasites & Vectors*, *8*(1), 135.

Waskom, M., Botvinnik, O., Gelbart, M., Ostblom, J., Hobson, P., & Lukauskas, S., Gemberline, D.C, Augspurger, T., & (2020). mwaskom/seaborn: v0. 11.0 (September 2020). *Zenodo*. https://doi.org/10.5281/zenodo.4019146

Weiss, S., Xu, Z. Z., Peddada, S., Amir, A., Bittinger, K., Gonzalez, A., Lozupone, C., Zaneveld, J. R., Vázquez-Baeza, Y., Birmingham, A., Hyde, E. R., & Knight, R. (2017). Normalization and microbial differential abundance strategies depend upon data characteristics. *Microbiome*, *5*(1), 27.

Welsh, R. M., Rosales, S. M., Zaneveld, J. R., Payet, J. P., McMinds, R., Hubbs, S. L., & Thurber, R. L. V. (2017). Alien vs. predator: bacterial challenge alters coral microbiomes unless controlled by *Halobacteriovorax* predators. *PeerJ*, *5*, e3315.

Welsh, R. M., Zaneveld, J. R., Rosales, S. M., Payet, J. P., Burkepile, D. E., & Thurber, R. V. (2016). Bacterial predation in a marine host-associated microbiome. *The ISME Journal*, *10*(6), 1540–1544.

Yilmaz, P., Parfrey, L. W., Yarza, P., Gerken, J., Pruesse, E., Quast, C., Schweer, T., Peplies, J., Ludwig, W., & Glöckner, F. O. (2014). The SILVA and "all-species living tree project (LTP)" taxonomic frameworks. *Nucleic Acids Research*, *42*(D1), D643–D648.

Zaneveld, J. R., McMinds, R., & Thurber, R. V. (2017). Stress and stability: applying the Anna Karenina principle to animal microbiomes. *Nature Microbiology*, *2*(9), 1–8.

Zhang, Y., Yang, Q., Ling, J., Van Nostrand, J. D., Shi, Z., Zhou, J., & Dong, J. (2016). The shifts of diazotrophic communities in spring and summer associated with coral *Galaxea astreata*, *Pavona decussata*, and *Porites lutea*. *Frontiers in Microbiology*, *7*, 1870.

SUPPORTING INFORMATION

Additional supporting information may be found online in the Supporting Information section.

How to cite this article: Brown T, Sonett D, Zaneveld JR, Padilla-Gamiño JL. Characterization of the microbiome and immune response in corals with chronic *Montipora* white syndrome. *Mol Ecol*. 2021;30:2591–2606. https://doi.org/10.1111/mec.15899